Acta Mechanica Sinica (2014) 30(4):526–532
DOI 10.1007/s10409-014-0057-2

RESEARCH PAPER

Highly reliable bipolar resistive switching in sol-gel derived lanthanum-doped $PbTiO_3$ thin film: Coupling with ferroelectricity?

Ying Wang · Wei-Jin Chen · Xiao-Yue Zhang · Wen-Jing Ma · Biao Wang · Yue Zheng

Received: 23 January 2014 / Accepted: 18 April 2014

Abstract Nanoscale $Pb_xLa_{1-x}Ti_{1-x/4}O_3$ (PLT) thin film has been fabricated on Pt\Ti\$SiO_2$\Si substrates by chemical solution deposition (CSD) method. Ferroelectricity of the fresh-made PLT thin film has been clearly detected through piezoelectric force microscopy (PFM) by writing reversible ferroelectric domains. However, PLT thin film also shows off-standard ferroelectric hysteresis loops highly dependent on frequency, indicating large amount of mobile space charges in the film. Subsequent current-voltage (C-V) studies show that sandwich-like Pt\PLT\Pt structure exhibits notable bipolar resistive switching (BRS) characteristics with high stability ($> 10^3$ switching cycles). It is found that the C-V curves of both high- and low-resistance states have the feature of space-charge-limited current (SCLC) conduction, indicating important roles of defects in the conduction. X-ray photoelectron spectroscopy measurement further verifies that oxygen vacancies based conductive filament mechanism is likely responsible for the observed RS effect. Our demonstration of stable RS effect in the PLT thin film and its possible coupling with ferroelectricity is promising in device development and applications, such as development of ferroelectric-tunable RS memories.

Keywords Ferroelectricity · Resistive switching · Stability · Oxygen vacancy

1 Introduction

Resistance random access memory (ReRAM), as a potential candidate for the next generation of nonvolatile memory, has attracted broad attentions due to its outstanding features such as simple capacitor-like cell structures, high storage density, high operation speed and low power consumption, etc. [1–10]. Various material systems have been demonstrated to possess resistive switching (RS) effect, including metal binary oxides such as ZnO, TiO_2, and NiO [1–3], perovskite oxides such as $BiFeO_3$ and $SrTiO_3$ [4, 5, 11], organic compounds [7], and SiO_2 [8], etc. Although there are still some controversies, several models have been proposed to explain the origins of RS effect, containing conductive filament model [11, 12], Schottky barrier model [5] and charge trap-detrap model [6] and so on.

On the other hand, ferroelectric thin films have been intensively investigated during the past decades, due to their prospective in device applications of nonvolatile memories, sensors, high-value capacitors, optical switches, and infrared detectors, etc. [13–19]. As one of the representatives, perovskite lanthanum-doped lead titanate $Pb_xLa_{1-x}Ti_{1-x/4}O_3$ (PLT) thin films have been widely investigated. They are well known to exhibit remarkable physical properties, including ferroelectricity, piezoelectricity, pyroelectricity, as well as excellent electro-optic and photostriction properties [20–23]. Among these properties, ferroelectricity in PLT

The project was supported by the National Natural Science Foundation of China (51172291, 11232015, and 11302267), the Fundamental Research Funds for the Central Universities, NCET in University, Research Fund for the Doctoral Program of Higher Education, Fok Ying Tung Foundation, Science and Technology Innovation Project of Guangdong Provincial Education Department, and Guangdong Natural Science Funds for Distinguished Young Scholar.

Y. Wang · W.-J. Chen · X.-Y. Zhang · W.-J. Ma · B. Wang (✉)$_2$ · Y. Zheng (✉)$_1$
State Key Laboratory of Optoelectronic Materials and Technologies, School of Physics and Engineering, Sun Yat-sen University, 510275 Guangzhou, China
e-mail$_1$: zhengy35@mail.sysu.edu.cn
e-mail$_2$: wangbiao@mail.sysu.edu.cn

Y. Wang · W.-J. Chen · X.-Y. Zhang · W.-J. Ma · B. Wang · Y. Zheng
Micro & Nano Physics and Mechanics Research Laboratory, School of Physics and Engineering, Sun Yat-sen University, 510275 Guangzhou, China

thin films has drawn special attentions for its important functionality and intimate connection with the composition and electro-mechanical characteristics of the film. In general, ferroelectricity of PLT thin film alters enormously depending on the amount of La doping. A larger La concentration tends to adjust the properties of PLT film closer to the ferroelectric-paraelectric phase boundary [24–27].

Recently, RS effect has been observed in ferroelectric thin films and has attracted increasing attentions [5, 6, 9, 11, 13]. It is natural to ask whether the RS behavior is or can be coupled with the intrinsic properties of the film, such as ferroelectricity. This coupling effect would be crucial to device performance and of great significance in revealing novel control strategies of RS effect, and provides us the possibility of developing tunable RS devices, e.g., ferroelectric-tunable RS memories. Nevertheless, to the best of our knowledge, few works have been reported about the RS effect in PLT thin films, not to mention the interaction between RS effect and other intrinsic properties such as ferroelectricity of the film.

Therefore, two questions arise, i.e., (1) whether PLT thin films possess RS effect, and (2) whether the RS effect (if exists) has influence on the other intrinsic properties of the film (especially ferroelectricity), and vice versa. To this end, we prepared PLT thin films with 5 mol% of La (i.e., $Pb_{1-x}La_xTi_{1-x/4}O_3$, with $x = 0.05$) and fabricate sandwich structures of Pt\PLT\Pt. Studies on ferroelectric properties, RS effect, as well as the relationships between them have been carried out on the samples. The PFM scanning results demonstrate strong ferroelectricity in the PLT films. Meanwhile, current-voltage (C-V) results show that the Pt\PLT\Pt structures exhibit typically reproducible bipolar resistive switching (BRS) characteristics. The conduction mechanism of the observed RS effect and its coexistence with ferroelectricity have been analyzed and discussed in this work.

2 Experiments

La-doped $PbTiO_3$ films with general chemical formula of $Pb_{1-x}La_xTi_{1-x/4}O_3$ ($x = 0.05$) were prepared by chemical solution deposition method (CSD) on Pt\Ti\$SiO_2$\Si substrates [22, 28, 29]. Lead acetate hydrate ($(CH_3COO)_2Pb{\cdot}3H_2O$), as one of the ingredients, was initially dissolved in acetic acid and stirred at 105°C for 15 minutes. After cooling to room temperature, the required quantity of titanium isopropoxide was added into the solution and mixed for several minutes. Lanthanum nitrate hydrate ($La(NO_3)_3 \cdot nH_2O$), which provides lanthanum, was introduced into 2-methoxyethanol and stirred at 60°C for 10 minutes. The solution were then mixed together and refluxed for several hours. Excess 5 mol% $(CH_3COO)_2Pb{\cdot}3H_2O$ was used to compensate the expected loss of volatile Pb during annealing process. Before spin-coating on the substrates, the solution was filtered to avoid particle contamination. The thermal treatment process for the samples was completed with a thermal annealing tube furnace. Firstly, the stoichiometric solution of PLT with concentration of 0.4 mol/L was spin-coated on the Pt\Ti\$SiO_2$\Si substrate at 420 r/min for 9 s and 3 500 r/min for 25 s. Then, the film was dried at 450°C for 5 min in air to remove volatile materials. These two processes were repeated several times to fabricate films with desired thicknesses. Finally, the films were annealed at 700°C for one hour in air ambient. Pt top electrodes with diameter of 0.3 mm were patterned on the films through ion sputtering system with a shadow mask. Hereto, the Pt/PLT/Pt structure was obtained.

The crystallinity and phases of the grown films were analyzed in θ–2θ mode by a Rigaku (D-MAX 2200VPC) X-ray diffractometer (XRD) with Cu Kα radiation ($\lambda = 0.154$ nm) at 40 kV and 30 mA. The cross-section and morphology structure of the pristine films were confirmed by Quanta 400F scanning electron microscopy (SEM) and CSPM5500 atom force microscopy (AFM). The polarization and domain properties of the films were studied through CSPM5500 piezoelectric force microscopy (PFM), and the polarization-voltage (P-V) hysteresis loops were obtained using an RT66 ferroelectrics test system (Radiant Technologies, USA). Current-voltage characteristics were measured by using a Keithley 4200 semiconductor characterization system (SCS) at room temperature. Chemical states of ions in the films were analyzed by X-ray photoelectron spectroscopy (XPS, ESCALAB250).

3 Results and discussion

The X-ray diffraction pattern for PLT thin film deposited on Pt\Ti\SiO_2\Si substrates is shown in Fig. 1a. The index Bragg reflections indicate that polycrystalline perovskite structure has been formed. No traces of impurity phases were found within the XRD detection limit. The schematic plot of Pt\PLT\Pt device is shown in the right above corner of Fig. 1a. The SEM cross section image of the film was studied to acquire the thickness of each layer, as shown in Fig. 1b. It could be clearly seen that PLT thin film has been well deposited on the substrates with thickness of ~ 200 nm. The AFM and SEM surface images of the film are shown in Figs. 1c and 1d, respectively. From these images, homogeneous crystal grains could be observed with the film surface root mean square (rms) roughness of about 8.43 nm and the average grain size about dozens of nanometers, revealing that a dense and smooth surface morphology was obtained in the derived PLT film.

At first, ferroelectric characteristics of the PLT film were investigated by PFM. As briefly shown in Fig. 2a, research was carried out on the exposed surface of PLT thin film without Pt top electrode. Gold-coated conductive probe of PFM, replacing the Pt top electrode, was utilized as a scanning probe and the top electrode. To see whether the PLT thin film is ferroelectric, we applied a voltage of −15 V to a particular region in the film to write domain pattern of "SYSU". The domain pattern was detected by the subse-

quent PFM scanning with a relatively small voltage of −2 V, and was characterized by the piezoelectric force signal. The written ferroelectric domain of "SYSU" was clearly seen, as shown in Fig. 2b. In the written area of "SYSU", the piezoelectric force signal was different from that of adjacent domains outside the written area, which results in distinguished bright area and dark area and indicates a sudden change of polarization direction. This result strongly indicates that the fresh-made PLT thin film exhibits ferroelectricity.

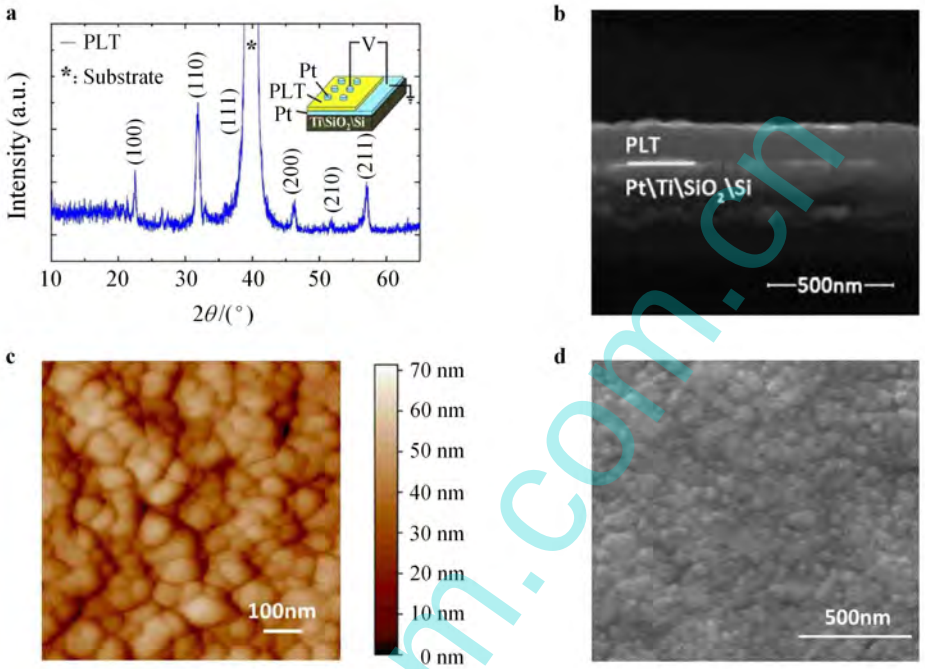

Fig. 1 **a** XRD pattern of Pt\PLT\Pt device, with an inset of the schematic diagram; **b** SEM cross-sectional image of Pt\PLT\Pt device; surface morphologies and grain sizes of PLT measured by **c** AFM, and **d** SEM

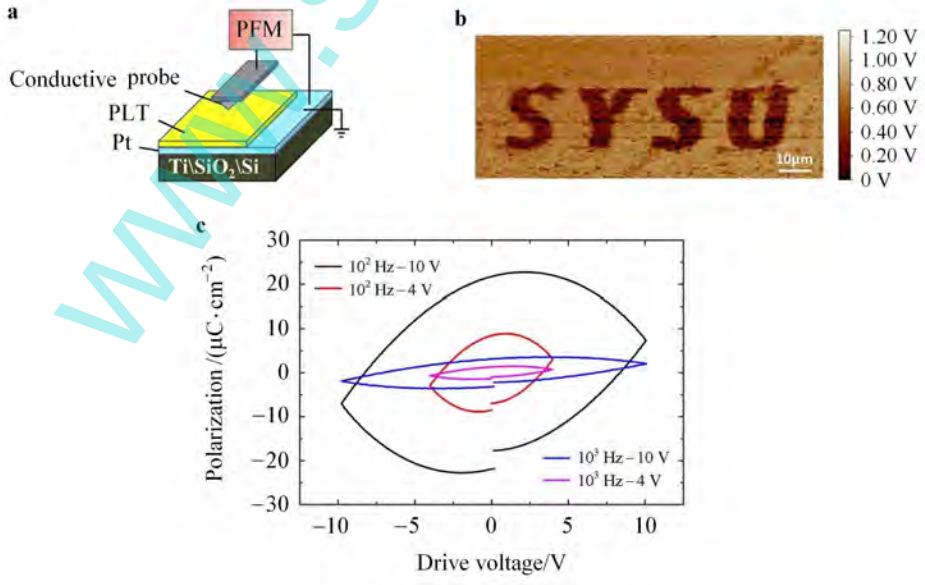

Fig. 2 **a** Schematic of PFM tests; **b** PFM images with written letters of "SYSU", where different domain directions are represented by the light and the shade areas; **c** P-V hysteresis loops of Pt\PLT\Pt device tested under different drive voltage and frequency, depicted by different colors

The ferroelectricity of PLT thin film has been further characterized through the measurement of the conventional hysteresis loop using an RT66 ferroelectrics test system. In contrast to the PFM result, we did not observe standard ferroelectric hysteresis loop on the sample. As shown in Fig. 2c, the "polarization"-voltage (P-V) loop is highly dependent on frequency and shows no saturated "polarization" at high voltage. The obtained hysteresis loops indicate large amount of mobile space charges and large leakage current in the sample. In the following, we will see that there are abundant oxygen vacancies in the PLT thin film actually. Because of oxygen vacancies, we believe that the PLT thin film can exhibit notable RS effect, as verified in the subsequent current-voltage (C-V) analysis. As indicated by the schematic plot in Fig. 1a, the C-V tests were started by applying a positive voltage on the top Pt electrode of the prepared device with a voltage increment of 0.02 V. The C-V characteristics of the device are illustrated in Fig. 3, where the data is plotted in semi-log scale. At the very beginning, the forming process was achieved when the device underwent a stepwise increase of voltage (until 8.3 V) for sufficient time, with a compliance current of 0.1mA to prevent the films from permanent breakdown, as shown in the inset of Fig. 3a. With regular voltage sweep of $0\,V \rightarrow +6\,V \rightarrow 0\,V \rightarrow -6\,V \rightarrow 0\,V$, more than one thousands of cycles of typical RS behavior were observed. The RS of our sample is bipolar, with opposite sign of the set voltage V_{set} and reset voltage V_{reset}. To see the stability of RS, the first fifty cycles and the last fifty cycles of the $> 10^3$ C-V sweeps were selected, and their absolute values are plotted in semi-log scale, with arrows indicating the direction of sweep voltage, as shown in Figs. 3a and 3c, respectively. It is apparent that V_{set} and V_{reset} presents large variation during the first fifty cycles, with V_{set} ranging from 1.6 to 5.8 V and V_{reset} ranging from 0.5 to 2.1 V (Fig. 3a). In the subsequent hundreds of switching cycles, the set-reset processes tend towards a stable state. For the last fifty cycles of which larger than $> 10^3$ C-V sweeps, the RS process has become quite stable with V_{set} of about 1.3 V and V_{reset} of about 0.9 V. To see the stable RS more clearly, one of the last fifty RS cycles has been individually picked out and depicted in the inset of Fig. 3c.

Furthermore, resistance evolutions of a high resistive state (HRS) and a low resistive state (LRS) in the first and the last fifty cycles of the device were calculated and plotted in semi-log scale, as shown in Figs. 3b and 3d. It is evident that resistance ratio exhibited a quite large variation in the first fifty cycles, which varied over almost four orders of magnitude in the initial twenty two cycles, and the variation gradually decreased to one order of magnitude in the following twenty eight cycles. On the contrary, as the blue fitting line shows, resistance ratio of HRS and LRS in the last fifty cycles exhibited relatively steady behavior, varying within one order of magnitude, which is considered to be related to the RS mechanism of the device (refer to the following). Therefore, throughout our C-V test, the Pt\PLT\Pt device stably maintained typical bipolar RS characteristics in more than one thousand C-V sweeps. To the best of our knowledge, it is the first time that such stable and reliable RS characteristics are found in ferroelectrics of PLT thin films.

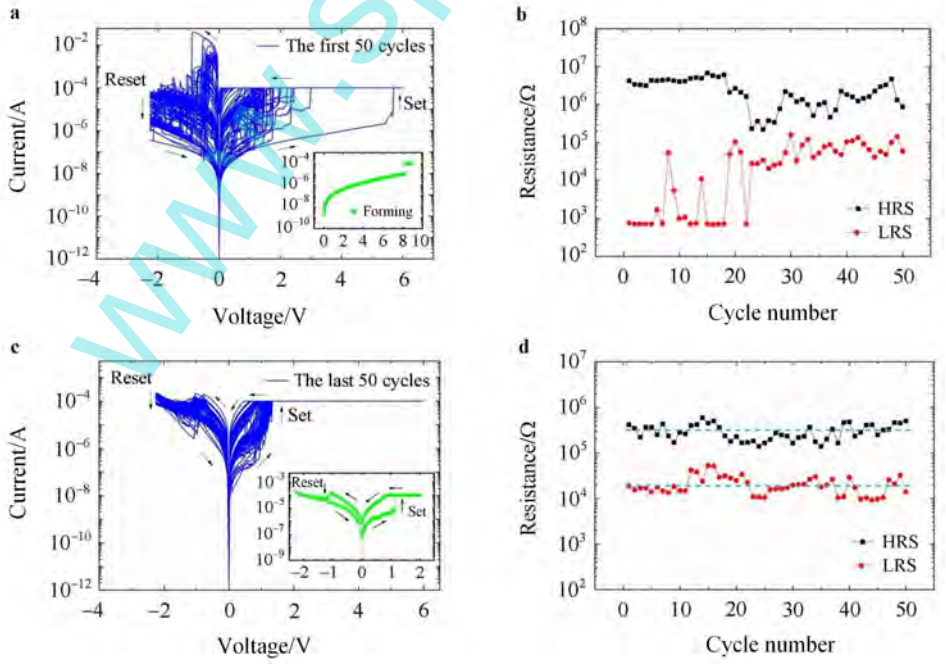

Fig. 3 The BRS current-voltage behaviors of Pt\PLT\Pt device in **a** the first fifty cycles, and **c** the last fifty cycles, with absolute values plotted in semi-log scale. The insets in right below corner of **3a** and **3c** show respectively the forming processes before BRS and a single BRS cycle picked out from the last fifty cycles. The resistance evolution of HRS and LRS in BRS process within **b** the first fifty cycles, and **d** the last fifty cycles, as plotted in semi-log scale

To further analyze the bipolar RS characteristics, one cycle of the last fifty C-V curves in Fig. 3c was chosen and replotted in logarithmic scale in Figs. 4a and 4b. From the linear fitting results with red lines, the slopes in set process are about 1.02 and 1.08 in low voltage region, while up to approximately 1.54 and 1.80 in high voltage region, as shown in Fig. 4a. Similarly, straight fitting lines with the slopes of ~1.06 and ~1.15 in low voltage region, together with ~1.98 and ~1.80 in relatively high voltage region, can be obviously observed in Fig. 4b. The results can be associated to space-charge-limited current (SCLC) theory [30, 31]. According to the typical SCLC theory, the concentration of injected carriers is lower than the thermal equilibrium carrier concentration in low voltage region, which will make the current behavior show Ohmic conduction property ($I \propto V^m$, $m \approx 1$). As the voltage increases to large enough value to make the density of injected carriers greater than the equilibrium number of carriers, the Ohmic conduction transitions to the trap-controlled conduction ($I \propto V^m$, $m > 1$), resulting in larger slope values in high voltage region. Since SCLC conduction mechanism is controlled by the localized traps of thin film, it is believed to be of great relevance to the RS behavior of the Pt\PLT\Pt device.

To clarify the type of traps in the PLT thin film, the chemical states of Pt ions, Ti ions and O ions have been investigated by X-ray photoelectron spectroscopy (XPS). The results of curve fitting was generated by subtraction of a Shirley background, followed by decomposition calculations using Gaussian–Lorentzian mixed functions [32]. The peak-fitted XPS spectrum is illustrated in Fig. 5. As shown in Fig. 5a, the spin-orbit split Pb (4f) peak exhibits only one binding states at Pb ($4f_{7/2}$) ~ 138.31 eV and Pb ($4f_{5/2}$) ~

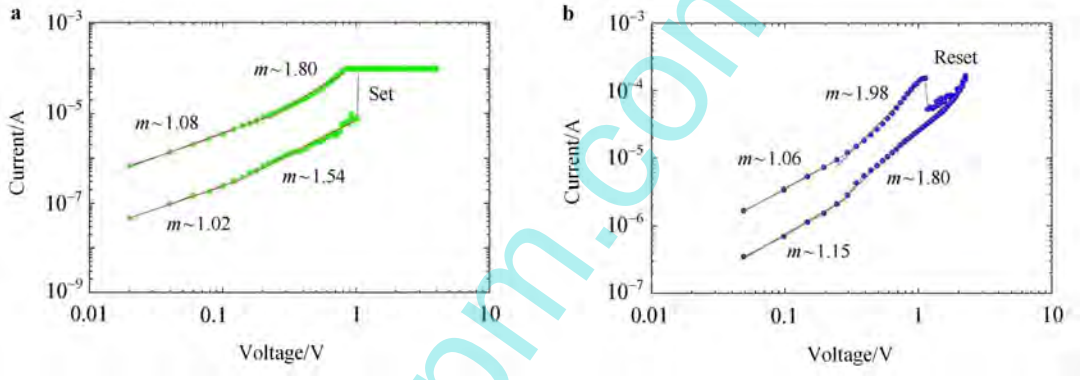

Fig. 4 The BRS current-voltage curves replotted in log-log scale. **a** Positive bias range; **b** Negative bias range

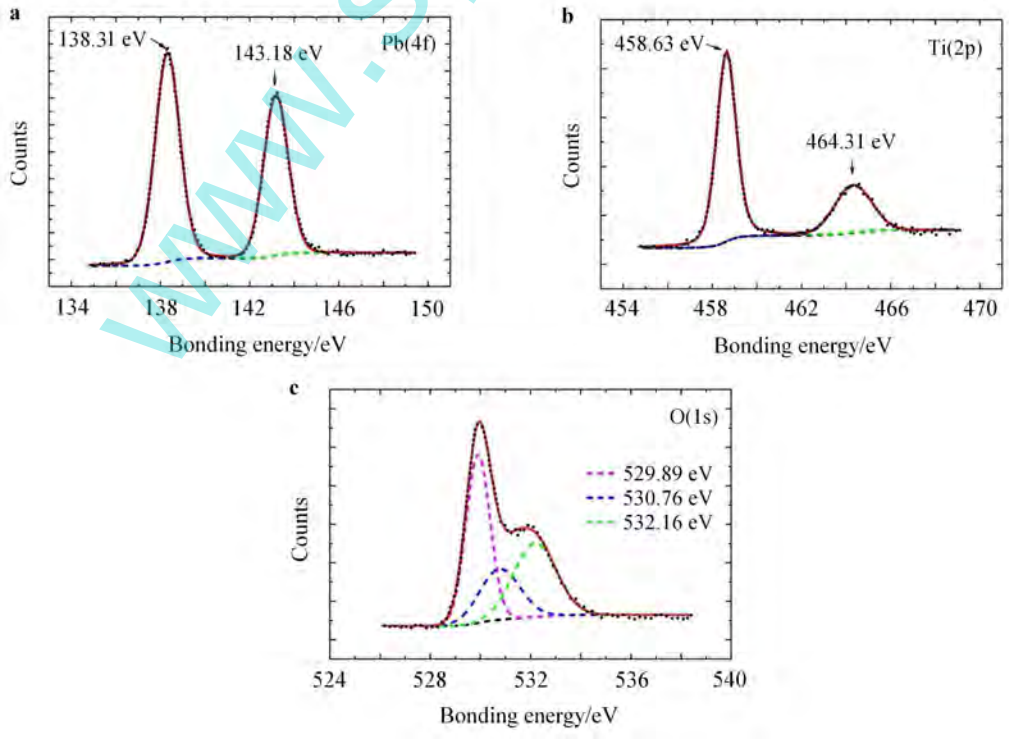

Fig. 5 XPS spectra of **a** Pb(4f), **b** Ti(2p), and **c** O(1s) in the PLT thin film

143.18 eV, which well corresponds to the state of lead in the perovskite lattice [33, 34], demonstrating that only one chemical state has been realized on the surface of PLT thin film. In the spectrum of Ti(2p) shown in Fig. 5b, the $Ti(2p_{3/2})$ and $Ti(2p_{1/2})$ peaks are observed at binding energies of 458.63 and 464.31 eV, associated with different state of Ti present in the sample, assigning to titanium of TiO and $PbTiO_3$, which indicates that perovskite structure has been generated in the film. Figure 5c shows that the O(1s) spectra exhibits three peaks. The peaks correspond respectively to the perovskite lattice oxygen at 529.89 eV (pink line), the oxygen vacancies at 530.76 eV (blue line) and the surface absorbed oxygen at 532.16 eV (green line) [33–36], indicating complicated states of oxygen in the film. The abundant surface absorbed oxygen would possibly act as an absorption source to absorb water, oxygen and even other small molecules from its surroundings [37], supplementing oxygen vacancies to the film. Therefore, the XPS result evidences the existence of large amounts of oxygen vacancies on the film surface, which can provide large quantity of trapping sites for electrons and contribute to the formation of conductive filament. Note that the signal of lanthanum was very small in our XPS result, which may be due to the low doping and a small detecting region of the sample. Moreover, because of the minute scale of the conducting path and the limitation of XPS detection, the direct observation of voltage-dependent dynamic and cyclic evolution of the filament change in RS should be further elaborated, and it would be a worthy topic for future investigation.

Based on the above mentioned, we suggest that the oxygen-vacancies based conductive filament mechanism is responsible for the observed RS effect in PLT. As the forming voltage is applied to the device, chemical reactions producing oxygen vacancies take place at the electrode/PLT interface. These excess oxygen vacancies (as confirmed by XPS shown in Fig. 5c), together with those already existing in the PLT film during the preparation stage, will migrate and accumulate from one electrode to another under the applied voltage.

To a certain time, a conductive path forms between the two electrodes, and the device appears in ON state (i.e., transforms from HRS to LRS). Because of the compliance current, the conductive filament may not completely form (i.e., it may continue to grow if a compliance current is set larger). When the applied voltage turns to reverse, opposite reactions and migration of oxygen vacancies will take place and the conductive filament probably breaks at the electrode/PLT interface [12, 38], making the device turn to OFF state with the transformation from HRS to LRS. Within the first tens or hundreds of RS cycles, due to the complex physical and chemical process in the films, the form-break process of the conductive filament is not well reproducible, resulting in fluctuation observed in Figs. 3a and 3b. As the RS process repeated, the transport of oxygen vacancies tends to be regular and the form-break processes in conductive filament also become stable, giving rise to the uniform RS behavior in the last cycles (Figs. 3c and 3d).

Finally, we would like to discuss about the coupling between ferroelectricity and RS effect in the PLT thin film. As already shown in Fig. 2b, fresh-made PLT thin film can exhibit ferroelectricity. However, ferroelectric signal of the sample was hindered after subsequent measurements of P-V loops and RS curves, indicating large effect of space charges on the behavior of ferroelectricity. The hindering of ferroelectric signal after these measurements is attributed to the large leakage current caused by the formation of conductive filaments. In other words, it seems that there is a tradeoff between ferroelectricity and RS behavior in the same sample. Nevertheless, on account of the difficulty in characterizing the dynamics of polarization relaxation and RS process, it is not clear whether these two phenomena can coexist in the same sample, and how they couple with each other. Intuitional results about mechanism analysis of the interactive influence between ferroelectricity and RS effects are scarce, which is worthy of investigation in near future.

4 Conclusions

In summary, ferroelectricity and RS effect have been investigated in a Pt\PLT\Pt sandwiched structure fabricated on $Pt\backslash Ti\backslash SiO_2\backslash Si$ substrates by chemical solution deposition methods. The fresh-made PLT thin film has been shown to be ferroelectric through piezoelectric force microscopy by writing reversible ferroelectric domains. It should be especially noted that, due to the effect of large amount of mobile space charges, the PLT thin film also exhibited off-standard ferroelectricity when we measured the ferroelectric hysteresis loops using a ferroelectrics test system. Meanwhile, highly reliable bipolar nonvolatile RS characteristics have been reported in 5 mol% La-doped PLT thin films. The C-V results show that the film presents highly stable RS behavior up to more than one thousand switching cycles. Based on current conduction analysis, trap-limited SCLC conduction mechanism is considered to be dominant in the whole RS process. According to XPS results, the oxygen-vacancies based conductive filament mechanism is likely responsible for the observed RS behavior. The apparent RS characteristics and the intrinsic ferroelectricity observed in the device may have significant impacts on each other. Nonetheless, the exact influencing mechanism between them needs further studies, which may provide a promising way to device development and applications, such as the development of ferroelectric-tunable RS devices.

References

1 Cao, X., Li, X., Gao, X., et al.: All-ZnO-based transparent resistance random access memory device fully fabricated at room temperature. J. Phys. D: Appl. Phys. **44**, 255104 (2011)
2 Waser, R., Aono, M.: Nanoionics-based resistive switching memories. Nature Mater. **6**, 833–840 (2007)

3 Ielmini, D., Nardi, F., Cagli, C.: Physical models of size-dependent nanofilament formation and rupture in NiO resistive switching memories. Nanotechnology **22**, 254022 (2011)
4 Choi, T., Lee, S., Choi, Y. J., et al.: Switchable ferroelectric diode and photovoltaic effect in $BiFeO_3$. Science **324**, 63–66 (2009)
5 Jiang, A.Q., Wang, C., Jin, K.J., et al.: A resistive memory in semiconducting $BiFeO_3$ thin-film capacitors. Adv. Mater. **23**, 1277–1281 (2011)
6 Choi, J., Kim, J.S., Hwang, I., et al.: Different nonvolatile memory effects in epitaxial $Pt/PbZr_{0.3}Ti_{0.7}O_{0.3}$/LSCO heterostructures. Appl. Phys. Lett. **96**, 262113 (2010)
7 Scott, J.C., Bozano, L.D.: Nonvolatile memory elements based on organic materials. Adv. Mater. **19**, 1452–1463 (2007)
8 Waser, R., Dittmann, R., Staikov, G., et al.: Redox-based resistive switching memories-nanoionic mechanisms, prospects, and challenges. Advanced Mater. **21**, 2632–2663 (2009)
9 Yang, C.H., Seidel, J., Kim, S.Y., et al.: Electric modulation of conduction in multiferroic Ca-doped $BiFeO_3$ films. Nature Mater. **8**, 485–493 (2009)
10 Valov, I., Waser, R., Jameson, J.R., et al.: Electrochemical metallization memories—Fundamentals, applications, prospects. Nanotechnoledge **22**, 254003 (2011)
11 Muenstermann, R., Menke, T., Dittmann, R., et al.: Correlation between growth kinetics and nanoscale resistive switching properties of $SrTiO_3$ thin films. J. Appl. Phys. **108**, 124504 (2010)
12 Waser, R., Aono, M.: Nanoionics-based resistive switching memories. Nature Mater. **6**, 833–840 (2007)
13 Luo, J.M., Lin, S.P., Zheng, Y., et al.: Nonpolar resistive switching in Mn-doped $BiFeO_3$ thin films by chemical solution deposition. Appl. Phys. Lett. **101**, 062902(2012)
14 Zheng, Y., Woo, C.H.: Giant piezoelectric resistance in ferroelectric tunnel junctions. Nanotechnology **20**, 075401 (2009)
15 Luo, X., Wang, B., Zheng, Y.: Tunable tunneling electroresistance in ferroelectric tunnel junctions by mechanical loads. ACS Nano **5**, 1649–1656 (2011)
16 Damjanovic, D.: Ferroelectric, dielectric and piezoelectric properties of ferroelectric thin films and ceramics. Rep. Prog. Phys. **61**, 1267 (1998)
17 Ramesh, R., Aggarwal, S., Auciello, O.: Science and technology of ferroelectric films and hetrostructures for non-volatile ferroelectric memories. Materials Sci. Eng. **32**, 191–236 (2001)
18 Muralt, P.: Ferroelectric thin films for micro-sensors and actuators: a review. Journal of Micromechanics and Microengineering **10**, 136 (2000)
19 Singh, R., Chandra, S.: Sol-Gel derived La modified PZT thin films: Structure and properties. Dielectrics and Electrical Insulation. **11**, 264–270 (2004)
20 Paz de Araujo, C.A., Cuchiaro, J.D., MeMillan, L.D., et al.: Fatigue-free ferroelectric capacitors with platinum electrodes. Nature **374**, 627–629 (1994)
21 Kwon, S.Y., Bae, J.I.: Pyroelectric properties of $PbTiO_3$/P(VDF-TrFE) 0-3 nanocomposite films. Industrial Electronics, 2004 IEEE International Symposium **1**, 55–57 (1998)
22 Majumder, S.B., Bhaskar, S., Dobal, P.S., et al.: Investigations on sol-gel derived lanthanum doped lead titanate (PLT) films. Integrated Ferroelectrics **23**, 127–148 (1999)
23 Hur, C.H., Han, K.B., Jeon, K.A., et al.: Enhancement of the dielectric properties of $Pb(La,Ti)O_3$ thin films fabricated by pulsed laser deposition. Thin Solid Films **400**, 169–171 (2001)
24 Roy, S., Majumder, S.B.: Recent advances in multiferroic thin films and composites. Journal of Alloys and Compounds **538**, 153–159 (2012)
25 Zhu, J., Wu, J., Xiao, D.: Growth and characterization of (Pb, La)TiO_3 films with and without a special buffer layer prepared by RF magnetron sputtering. Materials Letters **61**, 937–941 (2007)
26 Song, Z.T., W, H.L., Chan, C.L., et al.: Dielectric and ferroelectric properties of in-plane lead lanthanum titanate thin films. Microelectronic Engineering **66**, 887–890 (2003)
27 Song, Z., Ren, W., Fu, X., et al: Influence of Pb excess on the properties of lead lanthanum titanate ferroelectric thin films on Pt and $LaNiO_3$ electrodes. J. Phys.: Condens. Matter **13**, 155 (2001)
28 Koo, J., No, K., SooBae, B.: Synthesis and characterization of highly oriented Sol-Gel (Pb, La) TiO_3 thin film optical waveguides. Journal of Sol-Gel Science and Technology **13**, 869–870 (1998)
29 Di, W., Li, A.D., Ge, C.Z., et al.: Raman spectroscopy and X-ray diffraction study of sol-gel derived $(Pb_{1-x}La_x)Ti_{1-x/4}O_3$ thin films on Si substrates. Thin Solid Films **322**, 323–328 (1998)
30 Lamb, D.R.: Electric Conduction Mechanisms in Thin Insulating Films. Methuen, London (1967)
31 Hamann, C., Burghardt, H., Frauenheim, T.: Electrical Conduction Mechanisms in Solids. VEB Deutscher Verlag der Wissenschaften, Berlin (1988)
32 Shirley, D.A.: High resolution x-ray photoemission spectrum of the valence bands of gold. Phys. Rev. B **5**, 4709–4714 (1972)
33 Bhaskar, S., Majumder, S.B., Fachini, E.R., et al.: Influence of precursor solutions on the ferroelectric properties of Sol-Gel-derived lanthanum-modified lead titanate (PLT) thin films. Journal of the American Ceramic Society **87**, 384–390 (2004)
34 Chen, H.Y., Lin, J., Tan, K.L., et al.: Characterization of lead lanthanum titanate thin films grown on fused quartz using MOCVD. Thin Solid Films **289**, 59–64 (1996)
35 Bogle, K.A., Bachhav, M.N., Deo, M.S., et al.: Enhanced nonvolatile resistive switching in dilutely cobalt doped TiO_2. Appl. Phys. Lett. **95**, 203502 (2009)
36 Wakiya, N., Kuroyanagi, K., Xuan, Y., et al.: An XPS study of the nucleation and growth behavior of an epitaxial $Pb(Zr,Ti)O_3$/MgO(100) thin film prepared by MOCVD. Thin Solid Films **372**, 156–162 (2000)
37 Zheng, Z., Yuan, Y., Waclawik, E.R., et al.: Correlation of the catalytic activity for oxidation taking place on various TiO_2 surfaces with surface OH groups and surface oxygen vacancies. Chemistry **16**, 1202–1211 (2010)
38 Ma, W.J., Lin, S.P., Luo, J.M., et al.: Highly uniform bipolar resistive switching characteristics in $TiO_2/BaTiO_3/TiO_2$ ferroelectric multilayer. Appl. Phys. Lett. **103**, 262903 (2013)